Reduced Order Model for seismic analysis of geogrid reinforced soil walls

A. Carotti
Dept. of Structural Eng., Politecnico di Milano, Milano, Italy

P. Rimoldi
Tenax SpA,, Geosynthetics Technical Office, Milano, Italy

Laura Carozzi
Politecnico di Milano, Milano, Italy

Keywords: Design method, Geogrids, Numerical modelling, Seismic analysis, Walls

ABSTRACT: Within a research program started few years ago, the Authors present some recent results of the seismic dynamic modelling of tall geogrid reinforced soil walls.
A preliminary newtonian formulation of the analytical problem is explained, with a discrete model which yields the linear seismic dynamics of an unreinforced soil wall and the non-linear seismic dynamics of geogrid reinforced soil walls. Then a Reduced Order Model (ROM) is developed, based on the previous model, with concentrated inertia and elasticity. The MOR is validated through comparison with other reference models. The MOR allows to easy model, using a MATLAB software platform or similar ones, the seismic dynamic behavior of very tall walls, indicatively between 15 m and 30 m in height, which would require, with the previous model, a very high number of Degrees of Freedom (DOF), hence of differential equations.
The MOR is finally applied to a parametric analysis of the seismic dynamics of tall geogrid reinforced soil walls, and design charts are presented.

1 FULL ORDER MULTI DOF MODEL (ROM)

A non-linear multidof newtonian model for the seismic dynamics of slopes and walls on horizontally accelerated bedrock (Carotti and Rimoldi, 1997), is taken as the basic mathematical and computational support for developing a Reduced Order Model (ROM), suitable for numerical analysis of tall walls with high number of reinforcement layers.

From the multidof model, a series of 2-D response spectra and design charts have been obtained; from such plots the following kinematic and mechanical information can be deduced:
- maximum values of the seismic response at the top of the wall;
- spectral values of the active coefficient of earth pressure K_{agE} under seismic condition.

The mathematical model is based on the lumped mass scheme shown in Figure 1 and Figure 2.

The interactions between two adjacent masses is described in terms of two interlayers force fields: a conservative elastic field and a viscous-type field.

The Authors introduce the interlayers stiffness k_i, for the mass of thickness H_i and unit cross-section (that is for: L=D=1 in Figure 2):

$$k_i = \frac{\tau}{\gamma \cdot H_i} = \frac{G}{H_i} \tag{1}$$

and the interlayer viscous damping c_i:

$$c_i = \frac{\tau}{\dot{\gamma} \cdot H_i} = \frac{\overline{G}}{H_i} \tag{2}$$

where G is the elastic shear modulus, and γ is the shear strain (see Fig. 3.A)

From laboratory tests (Montanelli and Moraci, 1997), the Authors admit the following mechanical actions between the geogrids and the soil layers on top and bottom, as a consequesnce of the soil-geogrid interlocking.

1. An increase in the interlayer soil stiffness, proportional to the elastic stiffness of the geogrids. From monotonic tensile tests on geogrids the load÷strain curve has been reduced to a tri-linear curve and the stiffness value in each linear segment have been identified. Focusing the attention on the 1st stage, with strain threshold ε_I=0.03, if L_g is the geogrid length in the direction of the seismic acceleration, F is the tensile force applied to the geogrid and Δl its elongation, it is postulated that,
in condition of interlocking between geogrids and the soil layers, the contributed inter-layer stiffness is:

$$K_{g_i} = \frac{F}{\Delta l} = \frac{F}{\varepsilon_I \cdot L_g} \tag{3}$$

2. An increase of the interlayer viscous damping force, equal to the inherent viscous damping of the geogrid. From sinusoidal cyclic tests in geogrids with frequency f = 1.0 Hz and from the examination of an average elliptical cycle, the average viscous force F_{visc} (force in counterphase to the velocity, when the displacement is nil) has been obtained, together with the value of the peak velocity (product of the peak displacement, obtained from the test plot, and of the circular frequency ω = 2πf of the test). From the ratio force/velocity the damping coefficient is immediately obtained.
In details:

$$C_{g_i} = \frac{F_{visc}}{\Delta l \cdot \omega} = \frac{F_{visc}}{\varepsilon \cdot L_g \cdot \omega} \tag{4}$$

where Δ1 coincides with the differential interlayer displacement (x_i - x_{i-1}), when perfect interlocking between soils and geogrid has been assumed.

3. An increase of the interlayer damping due to the Coulomb friction between the geogrid and the soil layers, under the weight of the soil. The Coulomb friction due to the i-th geogrid (where N is the number of geogrid layers) is:

$$F_{Ci} = -tg\,\phi_{sg} \cdot g \cdot \sum_{k=i}^{n} M_k \cdot sign(\dot{x}_k)\ . \tag{5}$$

where the signum function $sign(\dot{x}_k)$ introduces the non linearity in the model. In Equation 5, ϕ_{sg} is the soil-geogrid interface friction angle; g is the gravity acceleration.

The Newtonian equations of motion for the N-DOF non-linear model with geogrids (N soil layers with N geogrid layers, see Figure 1 and 2) can be obtained taking into account the elastic stiffness K_{gi}, the viscous damping C_g and the Coulomb-type friction force F_{ci} induced by the geogrids.

Indicating with $\hat{M}$ the distributed load on top of the wall, the Newtonian equation of motion for the i-th layer is:

$$\begin{aligned} M_i \cdot \ddot{x}_i = \; & -K_i(x_{i-1}-x_i) - C_i(\dot{x}_{i-1}-\dot{x}_i) + K_{i+1}(x_i - x_{i+1}) + C_{i+1}(\dot{x}_i - \dot{x}_{i+1}) - \\ & -K_{g_i}(x_{i-1}-x_i) - C_{g_i}(\dot{x}_{i-1}-\dot{x}_i) + K_{g_{i+1}}(x_i - x_{i+1}) + C_{g_{i+1}}(\dot{x}_i - \dot{x}_{i+1}) + \\ & + tg\phi_{sg} \cdot g \cdot \left(\sum_{k=i}^{n} M_k + \hat{M} \right) \cdot sign\,\dot{x}_i - tg\phi_{sg} \cdot g \cdot \left(\sum_{k=i+1}^{n} M_k + \hat{M} \right) \cdot sign\,\dot{x}_{i+1} = \\ & = -M_i \cdot \ddot{x}_{br} \end{aligned} \tag{6}$$

where $g \cdot \left(\sum_{k=i}^{n} M_k + \hat{M} \right)$ represents the total gravity load acting on the i-th geogrid layer.

The steady dynamic equilibrium for a 1-DOF linear oscillator under 1-SIN resonant excitation is described in Figure 3.B in which the inertia force is balanced - at maximum displacement - by the elastic recalls.

In this non-linear model - (see Figure 3.B) - the contribution of the Coulomb friction force to the equilibrium (at maximum displacement) of the i-th layer of the wall, must be taken into consideration.

A geogrid reinforced earth wall is assumed, with a cohesionless backfill and possible permanent surcharge loads on the top surface; the vertical spacing S_V of the geogrids and the overall length L are taken as constant.

The following hypothesis are introduced:

- the static earth pressure P_{asi} is balanced even in seismic conditions by the Coulombian friction Fc_i and by the tensile strength Tg_i of the geogrids;
- in seismic conditions, the forces Fc_i furtherly provide an increase of damping (Equation 5), the forces Tg_i provide an increase in terms of damping (Equation 4) and stiffness (Equation 3);
- the dynamic earth pressure Pa_i can be obtained through the superposition of effects of the static earth pressure Pa_S and the seismic earth pressure Pa_{GE} (suffix “G” for geogrids and “E” for earthquake):

$$Pa_d = Pa_s + Pa_{GE} \tag{7}$$

- The earth pressures can be written according to the Rankine type equations:

$$Pa_d = \tfrac{1}{2}\, Ka_d\, \gamma\, H^2 \tag{8}$$

$$Pa_s = \tfrac{1}{2}\, Ka_s\, \gamma\, H^2 \tag{9}$$

$$Pa_{GE} = \tfrac{1}{2}\, Ka_{GE}\, \gamma\, H^2 \tag{10}$$

Therefore:

$$Pa_d = \tfrac{1}{2}\, (Ka_s + Ka_{GE})\, \gamma\, H^2 \tag{11}$$

$$Ka_d = (Ka_s + Ka_{GE}) \tag{12}$$

- due to the previous hypothesis, the dynamic forces can be studied independently from the static ones; therefore now on only the equilibrium of the dynamic forces will be considered.

The conditions of dynamic equilibrium and the mechanical interaction between the two adjacent layer (i-1)-th and i-th, are described in Figure 3.B, which gives an imagine at maximum displacement (zero velocity) of the wall. Being in conditions of zero velocity, at this point of time the viscous damping force Fv is zero. As above said, only the dynamic forces are considered, without the static earth pressure Pa_s.

Let F_{IN_i}; $Fe_{(i-l)}$; Fe_i represent, respectively, the overall inertia force and the elastic recalls above and under the i-th layer; and let $Fc_{(i-l)}$; Fc_i; P_{agE_i} represent the upper and lower Coulomb friction force and, respectively, the active earth pressure due to the i-th layer.
With the assumption that the 1st modal shape is dominating, then all the displacements of the single layers are in phase.
Hence there is a balance between the elastic recall forces of the soil itself; therefore Fe_i is almost equal to $Fe_{(i-1)}$ and computationally they can be neglected.
Under these hypothesis, in condition of dynamic equilibrium we have (see Figure 3.B):

$$P_{agE_i} = F_{IN_i} + T_{g_i}; \qquad F_{IN_i} = -M_i \cdot \ddot{x}_{si} \tag{13}$$

in which T_{g_i} means the tensile strength in the geogrid under the i-th soil layer (see Figure 4):

$$T_{g_i} = F_c \tag{14}$$

When the Rankine pseudo-static expression of Equation is introduced, a pseudo-static expression for the coefficient of active earth pressure K_{agE} under seismic excitation can be achieved:

$$k_{agE} = \frac{2 \cdot P_{agE}}{\gamma \cdot H^2} \tag{15}$$

The following classes of acceleration time histories have been implemented:

c1) a stationary gaussian zero-means white noise, low-pass filtered with fixed bandwidth (0 -5 Hz) and variable peak acceleration, with peak acceleration varying between 0.1 g to 1.1 g;

c2) as above but with parametrically fixed peak acceleration a_g= 5 m s^{-2} and variable bandwidth: all the bandwidths considered have the same left cut-off frequency (zero Hz) and different right cut-off frequencies, ranging from 1Hz to 7 Hz (or to 10 Hz for the case of wall with H = 3m). By this way the effects of many historic earthquakes can be modelled and simulated: from very low frequency “near-fault” earthquakes, to earthquakes with increasingly wider bandwidth, like the San Salvador (1986), Mexico City (1985) and El Centro (1940) records.

2 REDUCED ORDER MODEL (ROM)

2.1 *Parameters definition*

The number of non-linear equations describing the dynamics of the reinforced soil wall is equal to the number of soil layers used in the model, which in turn is equal to the number of reinforcement layers.

When the wall is very tall (say more than 15 m), the number of geogrid layers becomes very high, hence the numerical integration software (in this case the MATLAB platform) has to deal with a very big system of differential equation. This makes soon the numerical integration costly and unpractical, due to the type of computer and the running time required.

Therefore the Authors have developed a Reduced Order Model (ROM), which allows to decrease drastically the number of differential equations.

Let n be the number of equations and m a divider of n. The ROM consists in substituting m equations, related to m geogrid layers, with one equation related to an equivalent geogrid placed at the elevation of the center of gravity of the m layers.

For one geogrid to be equivalent to m ones, it is enough to reduce the interlayer stiffness to a $K_{gi_{ROM}}$ value, given by:

$$K_{gi_{ROM}} = \frac{1}{m} K_{gi} \qquad (16)$$

In such a way the number of equations is reduced m times.

Example:

a) for a wall with H=15 m, reinforced with geogrids equally spaced at 0.60 m centres, the thickness of each layer in the model is h=0.60 m, and the number of equations is n=25.
   Applying a ROM with m=2 gives n_{ROM}=13 equations.
b) for a wall with H=30 and h=0.60 m, it is n=50. With a ROM of order m=4 we obtain n_{ROM}=13 equations.

Even the damping C_{gi} of geogrids could be reduced in a similar way, but it has been checked that this parameter has not a big influence on the overall response of the ROM.

2.1 *Validation of the ROM*

The definition of the parameters of the ROM and the validation of the model have been carried out as follows:

1) the seismic linear dynamics of unreinforced tall walls has been studied with two models: the ROM and a continuous multi-modal model, used as a reference since it was previously validated; this latter model is a flexible vertical oscillator, locked at the base, with distributed inertia and elasticity.
   For both models the kinematic base excitation has been a mono-frequential (sinusoidal) horizontal motion at the bedrock: the frequency is slowly varied from static conditions to 4 Hz, while the acceleration is kept constant at 5.0 m/s^2.
   The results of this validation (see Figure 4) shows a very good agreement between the two models.
2) Two different models have been applied to geogrid reinforced walls with height H of 3.6, 6.0, 9.0, 12.0 m: the full order model explained at Par. 1 above, and a ROM with m=2. For all walls the following parameters have been used:
   - friction angle φ = 25°;
   - geogrid length = H .

The acceleration at the bedrock has been simulated with a gaussian noise, having a peak of 5.0 m/s^2 and flat PSD with different band amplitude for each case (left frequency equal to 0 Hz and right frequency equal to 6.5, 3.5, 3.0, 2.0 Hz respectively for the 3.6, 6.0, 9.0, 12.0 m high).

The geometrical and physical characteristics of the walls included in this study are reported in Tab. 1, while Tab. E provides thir modal characteristics.

The results of this comparison are shown in the same Figure 4.

The difference between the results of the full order model and of the ROM are in the range 10÷12%; hence the ROM can be considered a very good approximation of the full model.

3 CONCLUSIONS

Within the framework of a Newtonian model for the dynamics of a geogrid reinforced soil wall, a Reduced Order Model (ROM) has been developed, with the aim of providing a design method which could be implemented on a standard PC. The ROM allows to model even a very tall wall through a reduced number of differential equations, which can be solved numerically with a proper software (like the MATLAB platform used in the present paper).

The development of the ROM included two phases:

first the wall a non-linear lumped mass model is developed for both the reinforced and the unreinforced soil walls, and the inertia, elasticity and damping characteristics are set; this model is then subjected to simulated seismic actions and its numerical performances are checked;

then a criterion for condensing the lumped mass parameters is set, in order to get a reduced order model, which can be easily used for numerical computation of tall walls.

The ROM has been validated, even in modal sense, in both linear and non-linear conditions, against the first model, used as reference simulator.

The Authors wish to widen the scope of the ROM, to continue the validation process, and to extend its systematical use to the design process of reinforced soil walls in seismic conditions.

REFERENCES

Budhu M., Halloum H. (1994) "Seismic External Stability of Geotextile Reinforced Walls.", Fifth International Conference on Geotextiles, Geomembranes and Related Products, Singapore.

Carotti, A., Rimoldi, P. (1997) “Time and frequency domain models for the seismic analysis of geogrid reinforced soil walls. Proc. Geosynthetics '97 Conference, Long Beach, CA, USA

Montanelli F., Moraci N. (1997) "Behaviour of Geogrids under cyclic loads.", Proc. Geosynthetics’97, Long Beach, California, USA.

Murata O., Tateyama M. (1994) "Shaking table tests on a large geosynthetic-reinforced soil retaining wall model. Recent Case Histories of Permanent Geosynthetic-Reinforced Soil Retaining Walls", Tatsuoka & Leshchinsky Editors.

Table 1: Geometrical and physical characteristics of the walls

height	H		m	3	6	9	12	15	30
Length	L	H·3	m	9	18	27	36	45	90
Layer thickness	Hi		m	0.6	0.6	0.6	0.6	0.6	0.6
Soil density	ρ		Kgf*s2/m4	180	180	180	180	180	180
Mass	M	ρ·H·L·D	Kgf*s2/m	4.9·103	19.4·103	43.7·103	77.8·103	121.5·103	486·103
Elastic shear modulus	G		Kgf/m2	1.0·106	1.0·106	1.0·106	1.0·106	1.0·106	1.0·106
Viscous shear modulus	$\bar{G}$	G·α	Kgf*s/m2	2800	2800	2800	2800	2800	2800
Stiffness	Ki	G·L·D/ Hi	Kgf/m	15.0·106	30.0·106	45.0·106	60.0·106	75.0·106	150·106
Damping coefficient	Ci	$\bar{G}$·L·D/ Hi	Kgf*s/m	42.0·103	84.0·103	126.0·103	168.0·103	210.0·103	420·103
Friction angle	ϕ		rad	0.4363	0.4363	0.4363	0.4363	0.4363	0.4363
Direct shear factor	fds			0.8	0.8	0.8	0.8	0.8	0.8

Table 2: Modal characteristics of the walls

Height	(m)	3	6	9	12	15	30
1st mode	f1 (Hz)	5.6	2.9	2.0	1.5	1.2	0.6
	ξ1 (%)	4.91	1.29	0.58	0.33	0.21	0.05
	Γ1	1.27	1.27	1.27	1.27	1.27	1.27
2nd mode	f2 (Hz)	16.4	8.8	6.0	4.5	3.6	1.8
	ξ2 (%)	14.33	3.84	1.74	0.99	0.64	0.16
	Γ2	-0.42	-0.42	-0.42	-0.42	-0.42	-0.42
3rd mode	f3 (Hz)	25.9	14.4	9.9	7.5	6.0	3.0
	ξ3 (%)	22.60	6.30	2.88	1.64	1.06	0.26
	Γ3	0.24	0.24	0.24	0.24	0.24	0.24

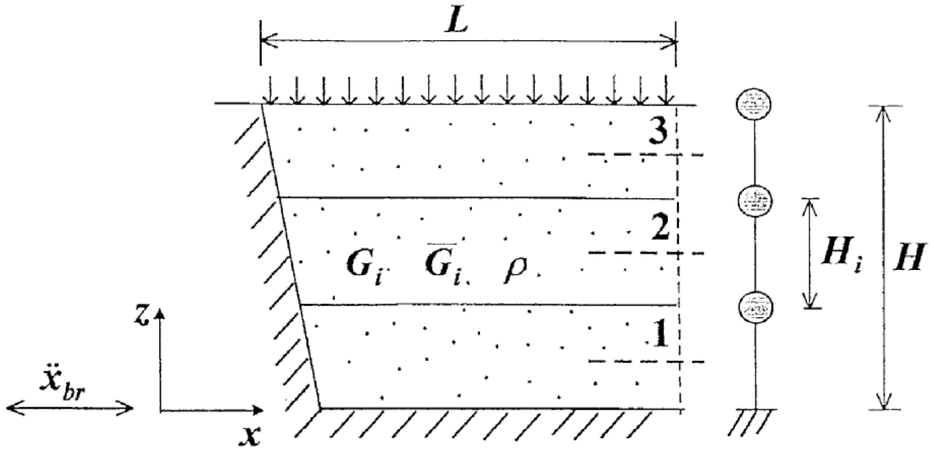

Figure 1: Scheme o the soil structure as a stack of layers and the lumped mass model.

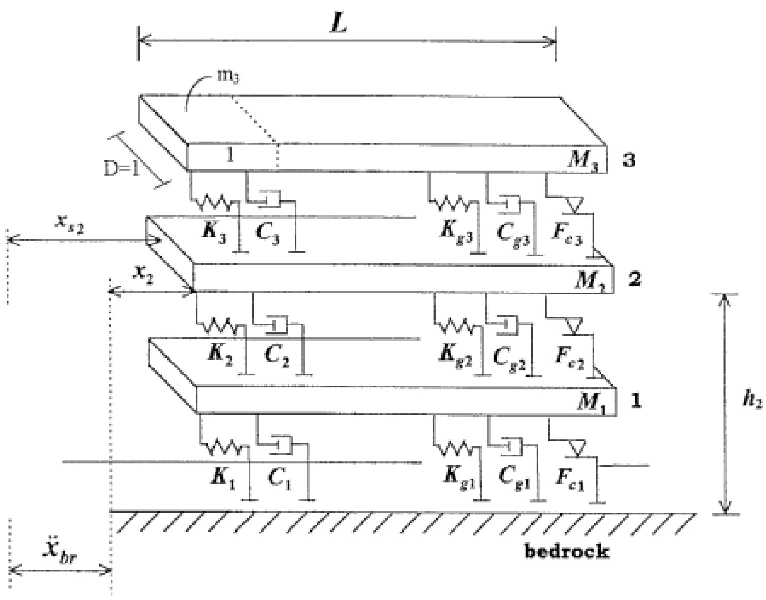

LEGEND:

M_i, K_i, C_i	mass, elastic stiffness and damping coefficient of i-th layer
K_{g_i}, C_{g_i}, F_{c_i}	elastic stiffness, viscous damping coefficient and Coulomb-type friction of geosynthetic-sheets
x_i, x_{s_i}	i-th layer dispacement: relative to bedrock, and absolute
$\ddot{x}_{br}$	bedrock acceleration
L, D	width and depth of embankment
h_i	height of i-th layer

Figure 2: The lumped mass model for a 3 DOF system, sowing all the interaction parameters.

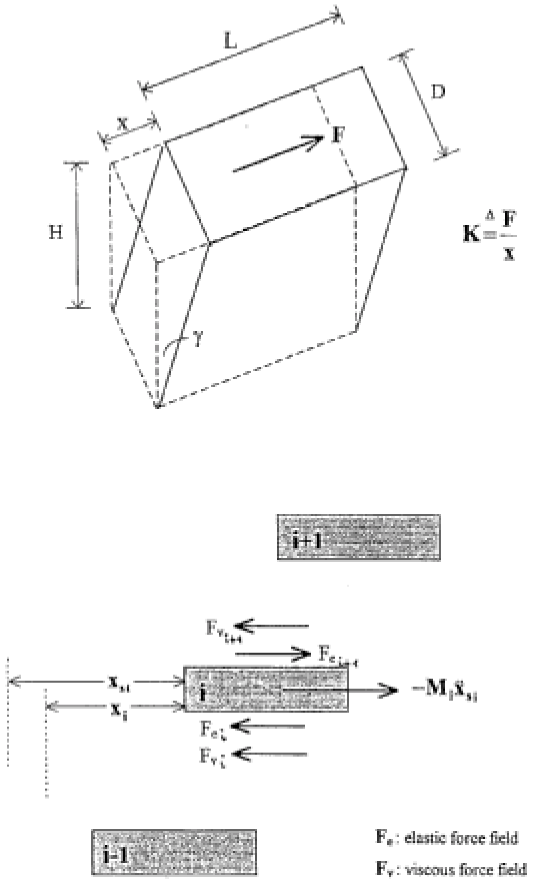

Figure 3: A) Scheme for the evaluation of the interlayer stiffness and viscous damping.
B) Scheme of the forces acting on a soil layer.

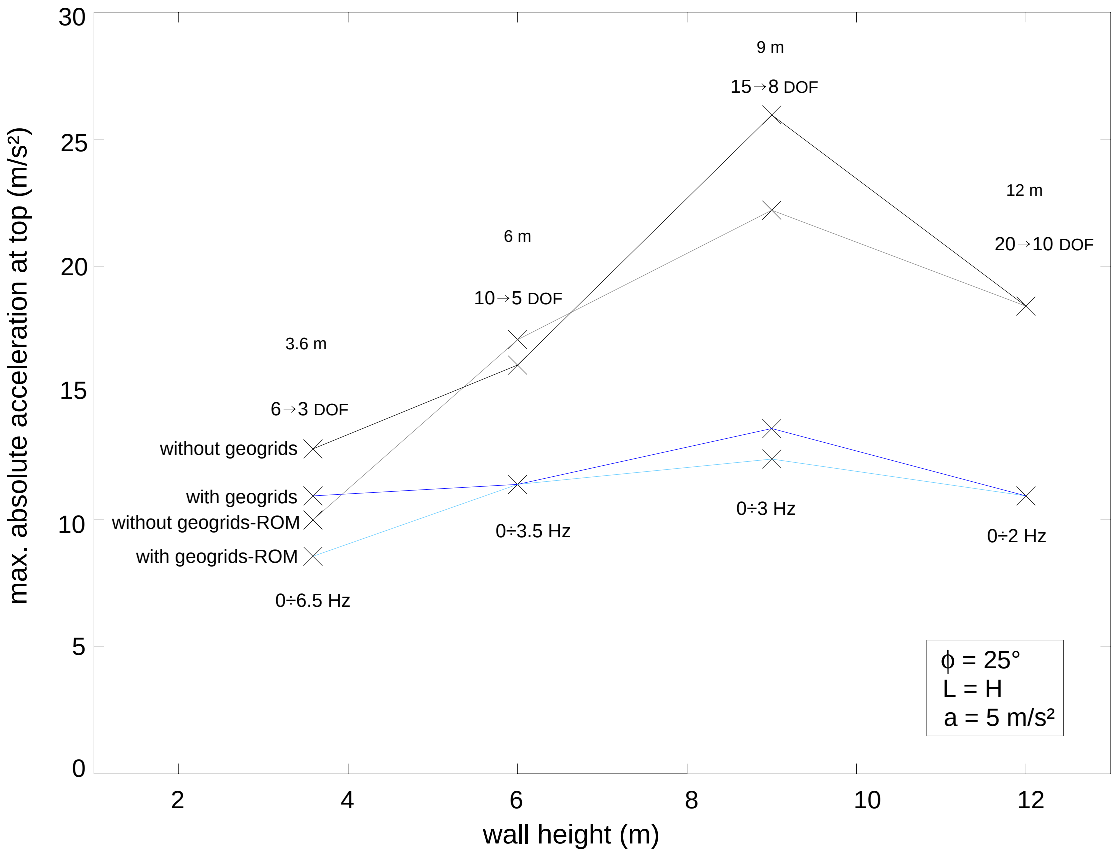

Figure 4: Validation of the ROM.